Astron. Astrophys. 350, 587–597 (1999)

ASTRONOMY AND ASTROPHYSICS

The Hipparcos HR diagram of nearby stars in the metallicity range: $-1.0 <$ [Fe/H] < 0.3

A new constraint on the theory of stellar interiors and model atmospheres

Y. Lebreton[1], **M.-N. Perrin**[2], **R. Cayrel**[2], **A. Baglin**[3], **and J. Fernandes**[4]

[1] DASGAL, CNRS URA 335, Observatoire de Paris, Place J. Janssen, 92195 Meudon, France (Yveline.Lebreton@obspm.fr)
[2] DASGAL, CNRS URA 335, Observatoire de Paris, 61 Av. de l'Observatoire, 75014 Paris, France
[3] DESPA, CNRS URA 264, Observatoire de Paris, Place J. Janssen, 92195 Meudon, France
[4] Observatório Astronómico da Universidade de Coimbra, 3040 Coimbra, Portugal

Received 26 March 1999 / Accepted 19 July 1999

Abstract. The Hipparcos mission has provided very high quality parallaxes of a sample of a hundred nearby disk stars, of spectral types F to K. In parallel, bolometric fluxes, effective temperatures, and accurate Fe/H ratios of many of these stars became available through infrared photometry and detailed spectroscopic analyses. These new accurate data allow to build the Hertzsprung–Russell diagram of stars of the solar neighbourhood with the smallest error bars ever obtained.

We analyse these observations by means of theoretical stellar models, computed with the most recent input physics.

We first examine the positions of the objects versus standard theoretical isochrones, corresponding to their chemical composition and age. For these isochrones we have first assumed that the helium content was varying in locksteps with metallicity. The comparison becomes age-independent in the lower part of the HR diagram, where evolutionary effects are negligible. We show that for the unevolved stars, the agreement between real stars and models is fairly satisfactory for stars with metallicity within $\pm$ 0.3 dex of the solar metallicity, but that a conflict exists for stars with metallicity less than [Fe/H] = -0.5. This conflict cannot be resolved by decreasing the helium abundance: values of this abundance below the primordial abundance would be required.

On the basis of recent works, we show that the addition of two processes not included in standard models can help solving the above discrepancy. These are (i) correcting the LTE iron abundances using a non-LTE approach and (ii) including microscopic diffusion of He and heavier elements in the stellar interior. The case of the binary star μ Cas is particularly useful to support this conclusion as its mass is also known from its orbit. After inclusion of the two effects, μ Cas A falls on its expected isochrone, within the error bars corresponding to its mass.

All stars with -0.3 $<$ [Fe/H] $<$ 0.3 are located between the helium-scaled isochrones corresponding to these metallicities. However five of them are not located exactly where they are expected to be for their metallicity. This may reflect a helium content lower than the metallicity-scaled value. But not necessarily, as a possible sedimentation of the elements might complicate the determination of the helium content. The age of main sequence solar composition stars covers a large range, and the effects of sedimentation are time dependent.

Key words: stars: abundances – stars: Hertzsprung–Russell (HR) and C-M diagrams – stars: interiors – stars: late-type – Galaxy: abundances – Galaxy: solar neighbourhood

1. Introduction

Valuable tests of the stellar evolution theory and strong constraints on the physical description of stellar interiors are mainly provided by the study of the most-accurately observed stellar objects. The number of observable parameters accessible through observations is important as well as the accuracy on their determination. The Sun, the nearby stars including members of visual binary systems, and stars belonging to open clusters represent some of these best-known objects.

The observations of nearby low-mass stars have been greatly improved, and their number has substantially increased, during the last few years. Distances have been determined with a very high precision with the Hipparcos satellite. In parallel, ground-based measurements have provided high resolution spectra and multicolour photometry of an appreciable number of stars of the solar neighbourhood. On the other hand, models of stellar atmospheres have largely benefited from progresses in the theoretical description of microscopic physics, in particular opacities. The analysis of the observational data, using model atmospheres, has provided bolometric magnitudes, effective temperatures and abundances with an accuracy which had never been reached previously. In addition, several nearby stars are members of visual binary systems and their mass is known.

The study of stars of low mass has many important physical and astrophysical implications. First, several uncertainties remain on the physics of their internal structure. For instance, the imperfect understanding of the convective transport or of

Send offprint requests to: Y. Lebreton

the non local thermodynamical equilibrium (non-LTE) effects in atmospheres and envelopes have important consequences: atmospheres and envelopes serve as external boundary conditions for the interior models, fixing the radius, and are also used in the analysis of observational data to determine abundances, effective temperatures and gravities. On the other hand, transport processes at work in the deep interior need to be better constrained; they link the convective zone to deep nuclear burning regions, involving consequences for the surface abundances (lithium and light elements but also heavy elements), and for the estimated age and global parameters, when fresh helium is brought to the burning core.

An important question is also that of helium content, not measurable in the photosphere due to the lack of lines in the spectrum. The initial helium content of a star determines its lifetime and internal structure and is also a witness of past galactic history. The knowledge of the initial helium abundance of stars born in different sites with different metallicities is therefore fundamental for studies of the chemical evolution of the Galaxy.

We study here a sample of a hundred nearby disk stars, of spectral types in the range F to late K, by means of theoretical stellar models. Our aim is to discuss the ability of the models to reproduce high quality observations and, when possible, to determine the helium content of the stars.

In Sect. 2 we make a rapid summary of some results previously obtained on the subject, from studies of a few particularly well-known objects. In Sect. 3 we carefully examine the observational data available for nearby stars in order to extract subsamples corresponding to the very best accuracies. We then present the derived Hertzsprung–Russell (HR) diagrams of stars of the solar neighbourhood which have the smallest error bars ever obtained. Sect. 4 describes the theoretical models used to compute isochrones for given chemical compositions. In Sect. 5 we show evidence for discrepancies between observations and theoretical models, which are particularly obvious for stars with metallicities below [Fe/H] =-0.5. In Sect. 6 we examine this problem in the light of recent works on departure from LTE for iron (Thévenin & Idiart 1999) and on microscopic diffusion of helium and heavier elements in metal-poor stars (Morel & Baglin 1999). We show that the cumulative effects of these two processes is large enough to remove the discrepancy shown in Sect. 5. Sect. 7 considers the case of binary stars with known dynamical masses. Sect. 8 addresses the question of the helium content of individual objects of the sample. Sect. 9 summarizes our conclusions.

2. Present status of helium content and mixing-length parameter determinations

Since observations do not provide direct determinations of helium, assumptions have to be made for the initial helium content of models of low-mass stars. Very often it is supposed that the metallicity Z and helium Y are related through a constant $\Delta Y/\Delta Z$-value.

$\Delta Y/\Delta Z = (Y - Y_{\rm p})/Z$ is often determined from the results of the solar calibration and for any other star of known metallicity, the helium abundance is scaled on the solar one. In addition of the behaviour of Y with Z, another problem is the universality of the $\alpha = l/H_p$ ratio of the mixing length over the pressure scale-height in the mixing-length treatment of the convection. We now briefly review the various determinations of these parameters, in the closest stars and various astrophysical sites.

2.1. Nearby stars

Perrin et al. (1977) were the first to examine the HR diagram of a selected sample of the nearest low-mass stars. Because in 1977 the error bars in the HR diagram were quite large, Perrin et al. (1977) suggested that all the non-evolved stars were sitting on the same ZAMS, whatever their metallicity was. They showed that this behaviour was reproduced by theoretical stellar models if helium and metallicity were related through a value of $\Delta Y/\Delta Z$constant and equal to 5. Recently Fernandes et al. (1996) claimed that stars do not all lie on the same ZAMS and measured the observational lower main sequence width in the solar neighbourhood. They showed that if the width is entirely due to chemical composition dispersion in the solar neighbourhood, then $\Delta Y/\Delta Z$is greater than 2 in the corresponding stars.

More recently Høg et al. (1997) and Pagel & Portinari (1998) have found $\Delta Y/\Delta Z = 3 \pm 2$ from a sample of nearby stars with Hipparcos parallaxes.

We recall further constraints on these points.

2.1.1. The Sun

The Sun is a milestone in internal structure theory, because its age and fundamental parameters are known with great accuracy, and helioseismology (Pérez Hernández & Christensen-Dalsgaard 1994) has brought additional constraints. All observations have to be reproduced by the theoretical solar model, with underlying input physics and free parameters. The *initial* helium abundance is a free parameter of the solar model and is estimated with the luminosity constraint (Christensen-Dalsgaard 1982). The difference between the present helium value derived from seismology($Y \approx 0.25$) and the initial value obtained from calibration ($Y \approx 0.275$) provides a constraint on the input physics of the model: it can be explained by invoking the microscopic diffusion of helium and heavy elements which has taken place during the evolution of the Sun (see e.g. Cox et al. 1989, Richard et al. 1996, Brun et al. 1998). Furthermore the mixing-length parameter, which enters the mixing-length phenomenology of convection is fixed by the radius constraint at a value $\approx$ 1.7–1.8.

2.1.2. Binary stars and clusters

The study of a few visual binary systems of known mass, effective temperature, luminosity and metallicity provides further information on low mass stars. The two components of a binary system, which are assumed to have the same age and initial

chemical composition, can be modelled simultaneously providing the age of the system, its initial helium content and the mixing-length ratio (Noels et al. 1991). The method was first applied to the α Centauri system by Noels et al. (1991). Recently, Fernandes et al. (1998) studied four Population I low mass binary systems with high quality data and determined the initial helium abundance by mass for three of them with a precision of 0.02. A global conclusion of these papers is that the mixing-length parameter α seems independent of metallicity, and that a $\Delta Y/\Delta Z$ratio of 2.3 ± 1.5 is appropriate (their Fig. 5).

Using the high quality observations of Hipparcos together with ground-based spectroscopic data, Perryman et al. (1998) and Lebreton et al. (1997) determined the helium abundance by mass, Y, of the Hyades with a precision of 0.02. This abundance does not follow the overabundance of the metallicity (+.15 dex). This suggests that a scatter does exist on the $\Delta Y/\Delta Z$ratio. This paper also confirms the universality of the α parameter.

2.2. Extragalactic observations

The studies mentioned above have provided the initial helium content of a few stars of known metallicity which allows to calculate their helium to metal enrichment ratio $\Delta Y/\Delta Z$= (Y - $Y_{\rm p}$)/Z. The primordial helium abundance Y_p has been determined by several groups: for instance, Balbes et al. (1993) gave $Y_{\rm p}$=0.227$\pm$0.006 while, more recently, Izotov et al. (1997) found a higher value $Y_{\rm p}$=0.243$\pm$0.003. However, Hogan et al. (1997) consider this value as an upper limit. This gives two secure points of the Y(Z) relationship: $Y_p \approx 0.24$ at $Z = 0.$, and $Y_\odot = 0.275$ at $Z = Z_\odot$. The observations of blue compact galaxies and other systems have allowed to determine a $\Delta Y/\Delta Z$ratio: a recent discussion is given by Thuan & Izotov (1998). The value is 2.3 $\pm$ 1.0, considerably below former determinations ≈ 4.0.

2.3. Nucleosynthesis

On the other hand nucleosynthetic predictions integrated over the whole stellar mass range lead to $\Delta Y/\Delta Z$-values ranging from about 1 to about 2 depending on the inclusion of stellar winds; $\Delta Y/\Delta Z$can even reach values of about 5 if black holes are considered (Maeder 1992). Although helium is expected to increase with metallicity, it must be noted that metals are only produced by SNe, whereas helium is also produced by mass-loss of medium-mass stars, in their post-AGB phase.

This body of results indicates that a significant dispersion of the helium abundance around the solar-scaled value cannot be excluded.

3. Observational determination of the stellar fundamental parameters

We study an homogeneous sample of 114 late-type nearby stars of spectral types in the range from F to late K, carefully selected by M.-N. Perrin. They are part of the proposal 132 (M.-N. Perrin), accepted as an Hipparcos program in 1982. Later on, the proposal was updated as the INCA proposal 011 by A. Baglin, M.-N. Perrin, Y. Lebreton and R. and G. Cayrel. These stars are closer than about 25 parsecs which ensures an excellent accuracy of their parallax determination by Hipparcos.

Among these, we have retained the stars which have been submitted to detailed spectroscopic analysis from the ground and which appear in the last version of the *Catalogue of [Fe/H] determinations: 1996 edition* by G. Cayrel de Strobel et al. (1997). Their metal to hydrogen ratio [Fe/H], i.e. the logarithm of the iron to hydrogen ratio (by number of atoms) relative to the solar value, ranges from about -1.0 to about +0.3 dex corresponding to Population I and thick-disk population. For each star we assign an averaged abundance determined from the above catalogue (for more details see the caption of Table 1). The mean internal error on [Fe/H] is of the order of 0.1 dex. This does not include systematic errors, as the fact that all abundances in the catalogue are not corrected for NLTE effects. In determinations based on spectra taken with solid state detectors, with high quantum efficiency, the random error coming from equivalent width measurements enters for about 0.03 dex only, the remaining part coming from uncertainties in the fundamental parameters $T_{\rm eff}$and $\log g$.

We eliminated the suspected unresolved binaries and only kept stars with parallaxes determined with an accuracy better than 5 per cent. Then, among the remaining stars, we extracted three homogeneous and independent subsamples.

Sample 1 is constituted of 33 stars with directly determined bolometric fluxes, so the problem of the value of the bolometric correction is eliminated. The relevant data for Sample 1 are listed in Table 1. The fluxes were derived by Alonso et al. (1995) with an accuracy of about 2 per cent by integrating UBVRIJHK photometry. The average absolute error on bolometric magnitude resulting from the parallax and bolometric flux uncertainty is of about 0.03 to 0.06 magnitude. The effective temperature was obtained by Alonso et al. (1996a) from the bolometric flux by the Infra-Red Flux Method (IRFM) (Blackwell & Shallis 1977). The method makes use of a grid of theoretical model line-blanketed flux distributions (Kurucz 1991). The mean internal error on effective temperature is about 80 K for temperatures greater than 4200 K (Alonso et al. 1996a). Fig. 1 shows the resulting positions of the stars in the (log $T_{\rm eff}$, $M_{\rm bol}$) diagram with their individual error bars. The striking feature of Fig. 1 is the lack of clear separation between stars having a solar metallicity, and those in the metallicity range [-1.0;-0.5], confirming with high quality data the result already obtained by Perrin et al. (1977), on less accurate data. In Fig. 2 the sample of stars plotted in Fig. 1 is split into 2 subsamples corresponding 1) to stars of solar metallicity, plotted in Fig. 2a and 2) to moderately deficient stars, plotted in Fig. 2b. Theoretical isochrones are also plotted in Fig. 2 but this will be discussed later in Sect. 5.

Sample 2 is constituted of 64 stars with effective temperatures derived from detailed spectroscopic analyses. For each star at least one determination of the effective temperature and of [Fe/H] was made with modern detectors (CCD or Reticon). We adopt a mean internal uncertainty on effective temperature of 150 K. Bolometric magnitudes were obtained using bolometric

Table 1. Observational parameters for Sample 1. Parallax π, and relative error on it σ_π/π come from the Hipparcos main catalogue. The apparent magnitude V is from the Hipparcos Input Catalogue. $M_{\rm bol}$ and $T_{\rm eff}$ were derived from the bolometric fluxes of Alonso et al. (1995, 1996a).Note that the zero-point of bolometric magnitudes is not that used by Alonso, but is such that M_{bol} =4.75 for the Sun. [Fe/H] values are a weighted average of individual values from spectroscopic analyses taken in Cayrel de Strobel et al. (1997). A quality index "qlt" was attributed to the adopted value of [Fe/H] according to the following code:

4: average of at least six determinations obtained with recent high S/N spectra
3: average of at least three determinations obtained with recent high S/N spectra
2: at least one determination obtained with recent high S/N spectra
1: [Fe/H] based on photographic spectra, keeping only high quality work, shown to be exempt of large systematic errors (often from Hernshaw, see Fuhrmann 1998)

HIC	HD	π	σ_π/π	V	$T_{\rm eff}$	$\sigma_{T_{\rm eff}}$	$M_{\rm bol}$	$\sigma_{M_{\rm bol}}$	[Fe/H]	qlt	
171	224930A	80.63	0.038	5.342	5562.	80.	5.220	0.087	-0.76	2	85 Peg
3821	4614	167.99	0.004	4.576	5817.	97.	4.506	0.031	-0.31	3	η Cas
5336	6582	132.40	0.005	5.789	5339.	82.	5.619	0.032	-0.76	2	μ Cas
7918	10307	79.09	0.010	4.451	5874.	99.	4.401	0.038	-0.02	3	
7981	10476	133.91	0.007	5.874	5172.	78.	5.694	0.033	-0.20	2	
8102	10700	274.17	0.003	5.680	5388.	81.	5.550	0.031	-0.56	4	τ Cet
10629	13783	25.82	0.041	5.360	5501.	86.	5.250	0.095	-0.55	1	
10644	13974	92.20	0.009	4.684	5591.	67.	4.594	0.036	-0.30	1	
13402	17925	96.33	0.008	6.040	5123.	75.	5.757	0.037	0.10	2	
16537	22049	310.75	0.003	3.726	5076.	86.	5.982	0.030	-0.17	3	ϵ Eri
17147	22879	41.07	0.021	4.758	5798.	87.	4.658	0.054	-0.88	4	
26779	37394	81.69	0.010	5.781	5185.	53.	5.611	0.037	-0.20	1	
27072	38393A	111.49	0.005	3.826	6260.	104.	3.806	0.032	-0.09	3	γ Lep A
36640	59984A	33.40	0.028	3.519	5928.	101.	3.429	0.068	-0.81	4	
39157	65583	59.52	0.013	5.863	5242.	59.	5.703	0.041	-0.61	1	
44075	76932	46.90	0.021	4.176	5727.	77.	4.106	0.054	-0.97	4	
50139	88725	27.67	0.037	4.960	5669.	66.	4.830	0.085	-0.65	-	
56997	101501	104.81	0.007	5.422	5342.	91.	5.312	0.034	0.03	1	
61317	109358	119.46	0.007	4.646	5867.	99.	4.586	0.034	-0.08	3	
64394	114710	109.23	0.007	4.452	5964.	93.	4.412	0.033	0.04	4	
70319	126053	56.82	0.018	5.043	5646.	68.	4.953	0.050	-0.20	2	
73005	132142	41.83	0.015	5.877	5098.	67.	5.697	0.044	-0.55	1	
73184	131977	169.32	0.010	6.864	4605.	43.	6.424	0.037	0.01	1	
80837	148816	24.34	0.037	4.212	5851.	62.	4.132	0.086	-0.80	3	
84478	156026	167.56	0.006	7.451	4345.	39.	6.881	0.033	-0.34	2	
88972	166620	90.11	0.006	6.174	4947.	74.	5.914	0.033	-0.20	1	
94931	+41 3306	28.28	0.030	6.097	5004.	139.	5.867	0.073	-0.87	2	
96100	185144	173.41	0.003	5.875	5227.	89.	5.705	0.031	-0.23	1	
96895	186408A	46.25	0.011	4.286	5763.	90.	4.226	0.038	0.06	2	16 Cyg A
96901	186427B	46.70	0.011	4.567	5767.	90.	4.487	0.039	0.06	2	16 Cyg B
98792	190404	64.17	0.013	6.317	5001.	75.	6.067	0.042	-0.15	1	
104214	201091A	287.13	0.005	7.490	4323.	50.	6.890	0.032	-0.05	1	61 Cyg A
114622	219134	153.24	0.004	6.497	4785.	59.	6.167	0.031	0.00	1	

corrections from Alonso et al. (1996a, 1996b), with a correction of the zero point giving a bolometric magnitude of 4.75 to the Sun. The resulting positions of the stars in the (log $T_{\rm eff}$, $M_{\rm bol}$) diagram are plotted in Fig. 3 and will be discussed later in Sect. 5.

Sample 3 is constituted of 15 stars with effective temperatures derived from the $(V-K)$ color index and from [Fe/H] according to the results from Carney et al. (1994), Johnson et al. (1966), Koorneef (1983). The mean internal uncertainty on effective temperature is of about 75 K. The bolometric magnitudes are derived from the V magnitude given in the Hipparcos input catalogue, using bolometric corrections from Alonso et al. (1996a, 1996b), with the same zero-point. Fig. 4 shows the resulting positions of the stars in the (log $T_{\rm eff}$, $M_{\rm bol}$) diagram with their error bars and will be discussed in Sect. 5. Very clearly Fig. 3 has a much larger scatter than Figs. 1, 2 and 4, showing that the effective temperatures derived from detailed analyses are not tightly connected to the true effective temperatures. The effective temperatures derived from $(V-K)$ on the contrary are tightly bound to those obtained by the IRFM, as it can be directly checked in the full Alonso sample. This is not surprising, as effective temperatures from detailed analyses are affected by other parameters: gravity, departures from LTE in ionisation

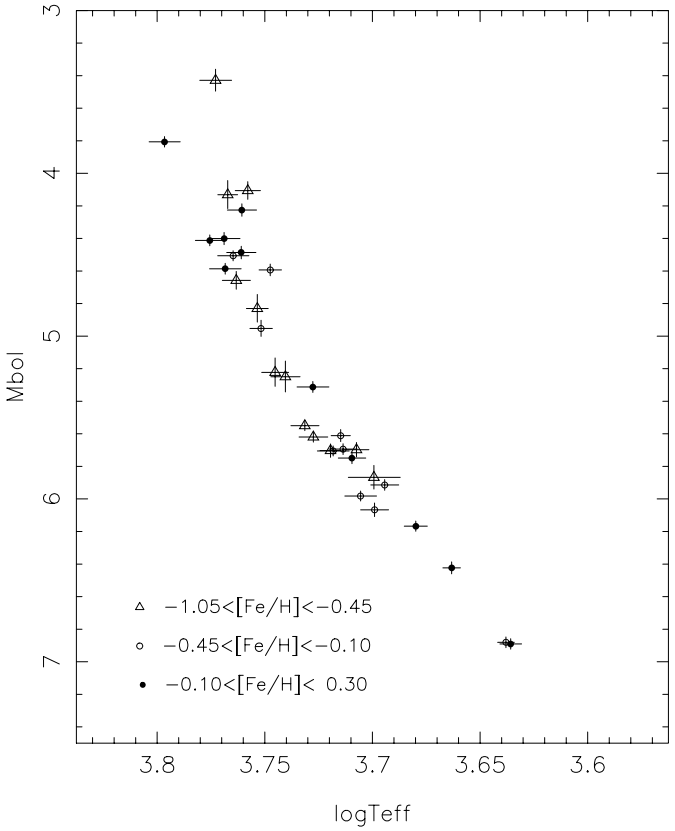

Fig. 1. The Hipparcos HR diagram of the 33 best known nearby stars (Sample 1, see text). The accuracy on the parallax is better than 5 per cent and bolometric fluxes are available for each star. Individual errors bars are given for each object by the horizontal and vertical sizes of the cross. Filled circles, open circles and open triangles respectively correspond to stars with [Fe/H] values in the interval [-0.10, 0.30], [-0.45, -0.10] and [-1.05,-0.45]

equilibria, and a variety of different techniques in fixing the triad ($T_{\rm eff}$, log g and [Fe/H]).

4. Theoretical stellar models

4.1. Input physics

The stellar evolution calculations were computed with the CESAM code (Morel 1997) in which we have included appropriate input physics for the mass range under investigation.

The CEFF equation of state (Eggleton et al. 1973, Christensen-Dalsgaard 1991), was used. It includes the Coulomb corrections to the pressure and is appropriate when modeling low-mass stars of mass greater than about 0.6 $M_{\odot}$(Lebreton & Däppen 1988).

We used the nuclear reaction rates given by Caughlan & Fowler (1988).

We calculated the initial composition of the models either from the Grevesse & Noels (1993) solar mixture (GN93 mixture) or from a GN93 mixture where the α-elements O, Mg, Si, S, Ca, Ti are enriched relative to the Sun ([α/Fe]= +0.4 dex). Such an enrichment of α-elements is observed in metal deficient stars with metallicities [Fe/H] lower than -0.5 (Wheeler et al. 1989, Fuhrmann 1998) and its effect on models has to be taken into account.

We took the most recent OPAL opacities (Iglesias & Rogers 1996) provided for the two mixtures considered. They were complemented at low temperatures by atomic and molecular opacities from Alexander & Ferguson (1994) for the GN93 mixture or from Kurucz (1991) for the α-enriched mixture. Low and high temperatures tables were fitted carefully at a temperature of about 10 000 K, depending upon the chemical composition.

In most models the atmosphere was described with an Eddington $T(\tau)$ law which is easy to use. In order to estimate the uncertainties resulting from this choice we built a few models using $T(\tau)$ laws derived from the ATLAS9 atmosphere models (Kurucz 1991). This requires to calculate detailed atmosphere models with ATLAS9 for many values of the gravity, of the effective temperature and of the metallicity and then to derive the corresponding $T(\tau)$ laws (see Morel et al. 1994). Interpolation of the $T(\tau)$ laws is then performed to model the considered star. We checked on a test-case, that the use of those better atmospheres does not shift the position of the model in the HR diagram by an amount larger than the observational error bars.

Convection was treated according to the mixing-length theory of Böhm-Vitense (1958). The mixing-length parameter α, ratio of mixing-length to pressure scale-height, is a free parameter of the models. As shown by Fernandes et al. (1998) the Sun and four visual binary systems spanning a wide range of masses and metallicities could be calibrated with very close values of α. Moreover the slope of the Hyades main-sequence is well-reproduced with a solar α-value (Perryman et al., 1998). On the other hand, Ludwig et al. (1999) made a calibration of the mixing-length based on 2-D radiation hydrodynamics simulations of solar-type surface convection and found that variations of α of about 10 per cent around the solar value are expected in the domain of effective temperature, gravity and metallicity studied here. We adopt the solar mixing-length value in our calculations. For unevolved stars a change of $\ell/H_{\rm p}$ of $\pm$ 0.15 produces a change in effective temperature of the order of 50 K, smaller than the mean observational error on $T_{\rm eff}$.

With the input physics described above the calibration in luminosity and radius of a solar model having $(Z/X)_{\odot}$ =0.0245, where X is the hydrogen abundance by mass (Grevesse and Noels 1993) requires a mixing-length $\ell = 1.64\ H_{\rm p}$, an initial helium abundance Y=0.266 and a metallicity $Z_{\odot}$=0.0175.

4.2. Grids of stellar models and isochrones

In order to determine the ZAMS position, we calculated zero and terminal age main sequences (ZAMS and TAMS) for 10 mass values ranging from 0.5 to 1.4 $M_{\odot}$, 5 helium values ranging from 0.18 to 0.43 and metallicities values Z= 0.004, 0.007, 0.01, 0.015, 0.02, 0.03, 0.04 and 0.06.

To discuss the global features of the HR diagram and the position of particular objects, we calculated detailed evolutionary sequences from the ZAMS to the beginning of the red-giant branch, for 14 masses ranging from 0.5 to 5 $M_{\odot}$and we derived

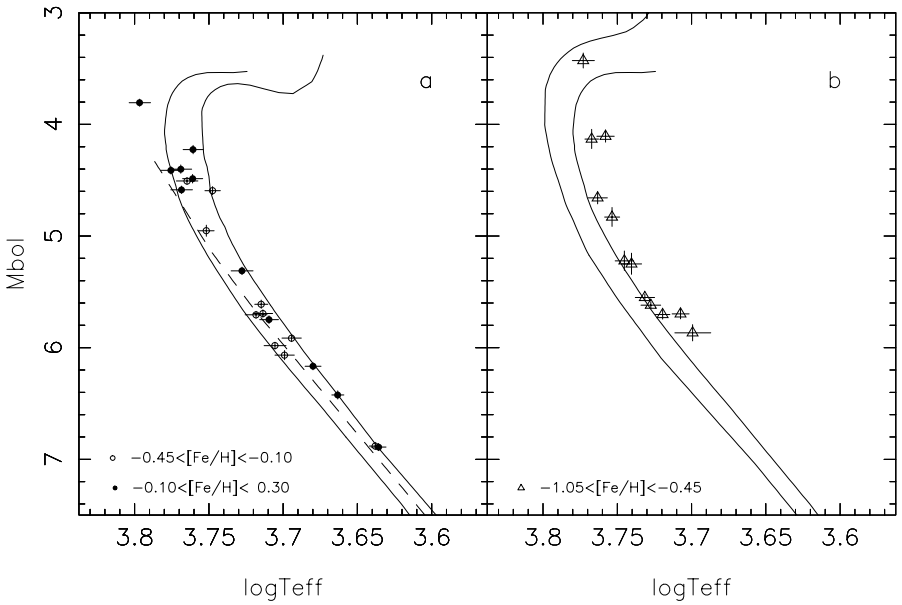

Fig. 2a and b. Same as Fig. 1 (i.e. stars of Sample 1) but split in two metallicity domains: stars of solar metallicity and close to it **a** and moderately deficient stars **b**. Theoretical isochrones are overlaid on the observational data. **a**: the lower isochrone (8 Gyr) is for [Fe/H]=-0.5, Y=0.256 and [α/Fe]=0.4; the upper isochrone (10 Gyr) is for [Fe/H]=0.3, Y=0.32 and [α/Fe]=0.0. The dashed line is a solar ZAMS. The young star γ Lep is the brightest star in the figure. **b**: the lower isochrone (10 Gyr) is for [Fe/H]=-1.0, Y=0.236 and [α/Fe]=0.4; the upper isochrone (10 Gyr) is for [Fe/H]=-0.5, Y=0.256, [α/Fe]=0.4. All stars, but one, are lying above the lane defined by these two isochrones.

isochrones using the Geneva isochrone program (Maeder 1974). We chose metallicities corresponding to the observational range (i.e. [Fe/H]=+0.3, 0.0, -0.5 and -1.0) and solar-scaled values of the helium abundance given by:

$$Y(Z) = Y_{\rm p} + (Z/Z_{\odot})\,(Y_{\odot} - Y_{\rm p})$$

with $Y_{\rm p} = 0.227$ (Balbes et al. 1993). This implies a $\Delta Y/\Delta Z$value of 2.2.

Two distinct grids of models were calculated in the metal deficient cases ([Fe/H] = -0.5 and -1.0): a grid with normal solar mixture and a grid with an α-elements enhancement of 0.4 dex. For the solar mixture grid the metallicity Z in mass fraction is related to [Fe/H] by:

$$[{\rm Fe/H}] = \log(Z/X) - \log\,(Z/X)_{\odot}$$

where $(Z/X)_{\odot}$ is the ratio of the solar mixture considered.

For the α -elements enhanced mixture the relation becomes:

$$[{\rm Fe/H}] = \log(Z/X) - \log\,(Z/X)_{\odot} - 0.305$$

where $0.305 = \log\,(Z/X)_{\odot,\alpha} - \log\,(Z/X)_{\odot}$, difference between a solar α-elements enhanced mixture and a 'normal' solar mixture.

The detailed results of all the stellar models computed for that work will be published separately (Lebreton et al., in preparation) and are available on request.

5. Comparison between theoretical isochrones and observational data

We present in Fig. 2a and in Fig. 2b the HR diagram of the 33 stars of Sample 1. We have split the sample in two subsamples: Fig. 2a corresponds to stars of solar metallicity or close to it ($-0.45 \leq [{\rm Fe/H}] < +0.30$) while Fig. 2b is constituted of the moderately metal deficient stars ($-1.05 \leq [{\rm Fe/H}] < -0.45$). We have superimposed on those diagrams theoretical isochrones associated to the limits of the metallicity ranges considered. Isochrones with [Fe/H] values of -0.5 and -1.0 have been derived from models calculated with an α-elements enriched mixture and have solar-scaled helium values, Y=0.256 and 0.236 respectively. The metal-rich isochrone has a solar α-elements ratio and Y=0.32. We have also plotted the position of the solar ZAMS on Fig. 2a. Isochrones are given for ages in the range 8–10 Gyr representative of the age of the galactic disk.

Fig. 2a shows that the stars of solar metallicity or close to it lie in the region defined by the theoretical models corresponding to their associated metallicity range. We notice the particular position of γ Lep (HIC 27072) which is a very young star lying close to the ZAMS.

However, it is worth to note that the slope of the theoretical main sequence agrees well with the observational slope. This, once more, is in favor of the uniqueness of the mixing-length parameter in low-mass stars. Furthermore the width of the global observed main-sequence band for metal-rich stars, which is around 0.3 mag, and the theoretical width corresponding to the same metallicity range with solar-scaled helium abundances are quite similar (see also Fig. 6).

Turning now to the moderately deficient stars plotted in Fig. 2b *we note that all the stars but one are outside the theoretical band corresponding to their metallicity*. Stars are located on theoretical isochrones with a metallicity higher than their observed metallicity.

The same behaviour is seen in the two other selected samples in which the effective temperatures of stars have been determined independently by different authors (see Sect. 3). Fig. 3a and 3b are similar to Fig. 2a and 2b but for the 64 stars with effective temperatures derived from detailed spectroscopic analysis (Sample 2) while Fig. 4a and 4b represent the situation of the 15 stars of Sample 3. Although the error bars on effective temperature are greater in Fig. 3a and 3b and although they are few objects in Fig. 4a and 4b, the same tendency is found, strength-

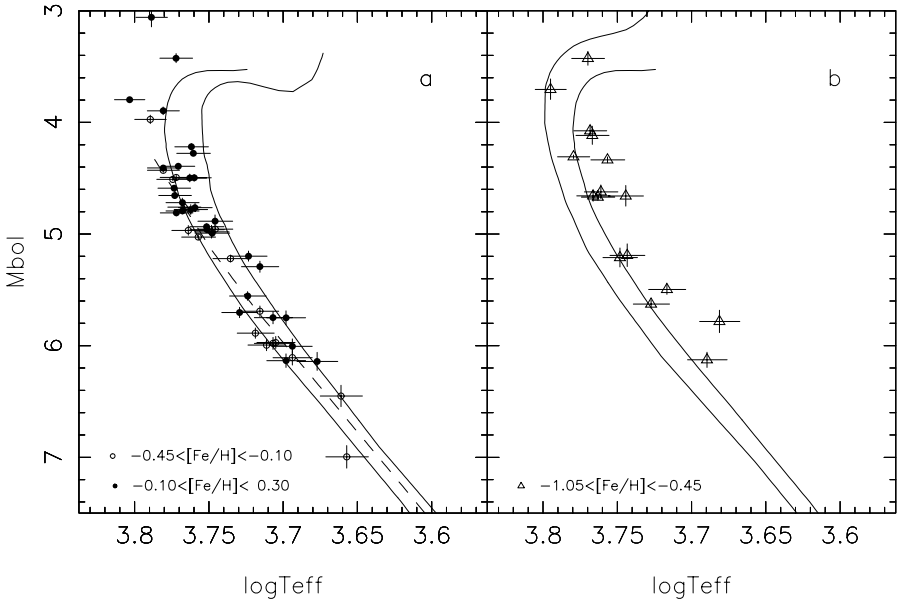

Fig. 3a and b. Same as Fig. 2 for stars of Sample 2 ($M_{\rm bol}$ is obtained from the Hipparcos parallax and V magnitude and $T_{\rm eff}$ from detailed spectroscopic analyses, see Sect. 3)

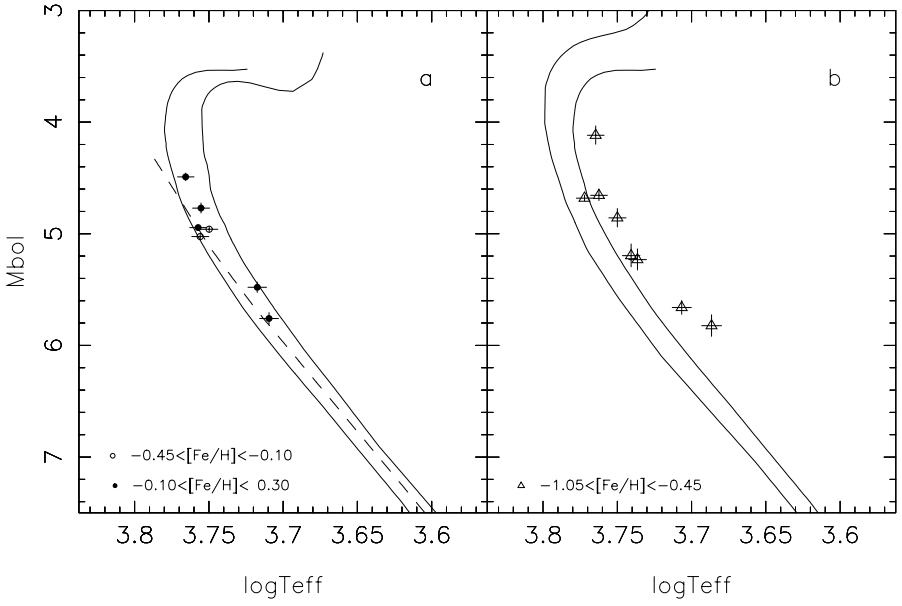

Fig. 4a and b. Same as Fig. 2 for stars of Sample 3 ($T_{\rm eff}$ is obtained from the (V-K) color index and from [Fe/H], see Sect. 3)

ening the conclusion that classical theoretical isochrones and actual observations of moderately metal deficient stars do not match.

Note that, in the confrontation of observational position of stars with stellar isochrones, errors on [Fe/H] and [α/Fe] which are in the range 0.10–0.15 dex, are responsible for a hidden enlargment of the error boxes, because the chemical composition of the models to be compared with the observed stars are not known exactly.

6. Resolving the metal-poor discrepancy

The most natural attempt to solve the discrepancy is by trying to adjust the "free" parameters, the helium content Y being the first target. However, for the stars in the metallicity bin $[-1.05, -0.45]$, a $\mathrm{Y} \leq 0.2$ would be required, a cosmologically unacceptable value. A change in $\alpha = \ell/\mathrm{H_p}$ does not help either, as it is producing a negligible effect in the low part of the main sequence under consideration here.

So, as noted in Lebreton et al. (1997) the discrepancy in the expected and actual positions of metal-poor stars needs either a drastic change in the zero-point of effective temperature (of the order of 200 K) or accepting the view that other processes must be included in the interpretation of the observations. It would be very difficult to plead a large correction in the effective temperatures at metallicity $[\mathrm{Fe/H}] = -0.7$ and none at solar metallicity. So, we do not further consider this explanation and, now focus on the second one.

Two processes are considered in this section: (i) departures to LTE in the determination of [Fe/H] (ii) microscopic diffusion of helium and other heavy elements.

6.1. Non-LTE departures for iron

All the [Fe/H] values we have used were computed with the LTE approximation. Computing NLTE abundances for iron is a formidable task. However, it must be noted that Bikmaev et al. (1990) have claimed that a substantial overionisation occurs for Fe I in subdwarfs, and only Fe II lines should be used for determining iron abundances. Holweger and coworkers (private communication, 1993) found the same phenomenon in trying to compute departures from LTE for the very metal-poor star $\mathrm{CD}-38°245$. More recently, Nissen et al. (1997) found that spectroscopic gravities in subdwarfs were systematically lower than the gravities derived from Hipparcos distances. Finally, Thévenin & Idiart (1999) have undertaken NLTE computations of iron abundances in one hundred metal-poor stars, and found non-LTE corrections for several of our stars, of the order of 0.15 dex, for the mean metallicity ($[\mathrm{Fe/H}] = -0.72$) of our $-1.05 \leq [\mathrm{Fe/H}] < -0.45$ subsample. Non-LTE corrections are negligible for stars with solar metallicities (same reference). The metallicity of isochrones to be compared to the set of stars with a mean LTE metallicity [Fe/H]=-0.72 is therefore the true NLTE metallicity [Fe/H]=-0.57. The situation is improved but a clear departure is still existing (Fig. 5).

6.2. Sedimentation of heavy elements

The effects of sedimentation of heavy elements have recently been computed by Morel & Baglin (1999), for stars of metallicity $[\mathrm{Fe/H}] = -0.7, -0.9, -1.2, -1.7$, and for 5 stellar masses, 0.85, 0.80, 0.75, 0.70, and 0.60 $M_\odot$. To produce significant effects in the HR diagram microscopic diffusion has to proceed on a sufficiently long timescale. This condition is fulfilled for the thick disk subsample under consideration here: the 10 Gyr isochrones of the Morel & Baglin paper are a suitable choice for our subsample. Two effects are present:

After a time of 10 Gyr, the stratification of the heavy elements translates the evolution point in both $\log T_{eff}$ and M_{bol}. This effect is small: at 0.7 $M_\odot$ and an initial metallicity of $[\mathrm{Fe/H}] = -0.75$ the point is moved by $\Delta M_{\mathrm{bol}} = -0.029$ and $\Delta \log T_{\mathrm{eff}} = -0.0004$. But the surface metallicity of the star has dropped to $[\mathrm{Fe/H}] = -0.81$. Therefore, the theoretical position of a star of present metallicity $[\mathrm{Fe/H}] = -0.75$, must be computed with a modified initial composition, leading after a 10 Gyr evolution, to the metallicity we observe now. This is the largest part of the correction, called the calibration correction by the authors. From their Table 2, and their Fig. 5 we have computed the corrections to be applied to a standard isochrone for the mean metallicity ($[\mathrm{Fe/H}] = -0.72$) of our sample in the range $-1.05 \leq [\mathrm{Fe/H}] < -0.45$.

6.3. Cumulated effect

Applying these corrections to the dashed curve in Fig. 5 produces the dot-dashed isochrone. No systematic departure appears any more between the observations and the theoretical isochrone corresponding to the present surface metallicity of the stars. The initial discrepancy noted at the beginning of this section is then completely removed. The only star presenting a 2σ discrepancy is the star HD 132142 at (3.707, 5.697). But there is a single spectroscopic determination of its metallicity and its photometry indicates a solar metallicity. So this exception is not a serious worrying.

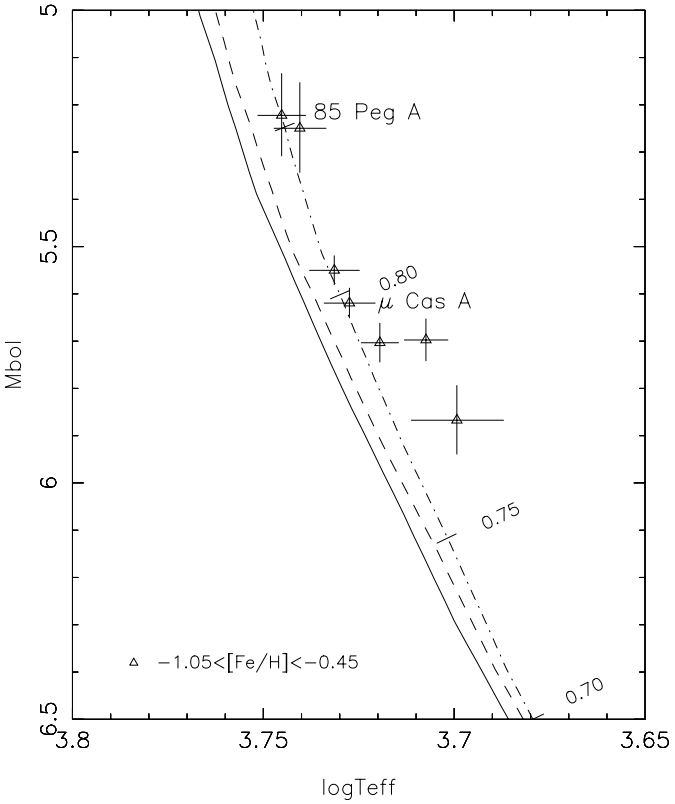

Fig. 5. This figure is a large scale HR diagram for the subsample of unevolved stars in the LTE metallicity range -1.05 < [Fe/H] < -0.45. The full line is a standard isochrone for the mean LTE metallicity of the sample [Fe/H] = -0.72. The dashed line is the standard isochrone corresponding to the NLTE mean metallicity of the sample [Fe/H] = -0.57. The dot-dashed line corresponds to an isochrone including microscopic diffusion of the elements for an age of 10 Gyr. The surface metallicity is the NLTE value [Fe/H]=-0.57, but the initial metallicity, which is very close to the mean interior metallicity was $[\mathrm{Fe/H}] \approx -0.5$. The fit is now satisfactory. The tick marks show the value of the mass along the upper isochrone. The tick mark near 85 Peg A corresponds to 0.85 $\mathrm{M}_\odot$ (not labeled for clarity)

7. Binary stars

One more constraint can be obtained from the stars of the sample which are component of a binary system having known orbit and masses. One of us (JF) has already used a few of the best known binaries in order to check the predictions of theoretical evolution computations (Fernandes et al. 1998). It is worth to see if, when known, the dynamical mass of the object confirms, or disproves, its location along the proper isochrone obtained above. The most interesting case is the binary μ Cas, the only metal-poor star, having a well determined mass.

Table 2. budget of the impact of parameter variations on the position of a star like μ Cas in the HR diagram. The reference model has an age of 12 Gyr, a mass of 0.757 $M_{\odot}$, Y = 0.245, [Fe/H] = -0.86, and [α/Fe]= 0.3 dex

parameter	increment	$\delta \log T_{eff}$	δM_{bol}
mass($M_{\odot}$)	0.06	0.031	-0.607
age (Gyr)	2	0.005	-0.150
Y	-0.015	-0.012	0.172
[Fe/H] (dex)	-0.15	-0.015	0.188
[α/Fe] (dex)	0.10	-0.004	0.064
α (MLT)	-0.15	-0.004	0.004
atmosphere	Eddington/Kurucz	-0.001	0.001
diffusion	yes/no	-0.007	0.040
low-T opacity	+30 per cent	-0.049	0.742

7.1. μ Cas

Drummond et al. (1995) have derived the mass of μ Cas from its orbit, with the help of speckle interferometry to see its very faint companion ($\Delta m \approx 5.0$). The mass of μ Cas A, readjusted with the better distance provided by Hipparcos is 0.757 $\pm$ 0.06 $M_{\odot}$. The Alonso et al. (1996a) effective temperature for (A+B) is 5315 $\pm$ 82 K, which corrected for the presence of the companion becomes 5339 $\pm$ 85 K, in good agreement with Fuhrmann (1998) effective temperature of 5387 $\pm$ 80 K. We obtain $\mathrm{M_{bol}} = 5.634 \pm 0.035$ for μ Cas A from its parallax, and again correcting for the presence of the companion. The position of the star is plotted with respect to the uncorrected and corrected isochrones in Fig. 5. The evolutionary masses along the dot-dashed isochrone are shown with tick-marks. The location of μ Cas is near 0.8 $M_{\odot}$, within the limits of the dynamical mass 0.757 $\pm$ 0.06 $M_{\odot}$. Unfortunately, the error bar on the mass is still a bit large to add an interesting new constraint. The influence of the uncertainties on the values of the various parameters of the models on the position of μ Cas in the HR diagram are documented in Table 2 (see Lebreton 1999 for more details).

7.2. 85 Peg

Fernandes et al. (1998) showed that, using the data available on this object, there was no theoretical solution fitting the two components. Later on, Martin & Mignard (1998), have restudied several binaries from Hipparcos data, and shown that it is very difficult to escape the conclusion that the mass of the primary and the secondary are very similar, notwithstanding the fact that the secondary is 3.2 magnitude fainter than the primary. New determinations of the effective temperature of 85 Peg A by Thévenin & Idiart (1999) and C. Van't Veer (private communication, 1998) confirms that 85 Peg A has a metallicity very similar to that of μ Cas A, an effective temperature of 5550 $\pm$ 100 K, and $\mathrm{M_{bol}}$=5.22 $\pm$ 0.06. Its location in the HR diagram (Fig. 5) is pratically on the same isochrone as μ Cas, and corresponds to a mass of 0.85 $M_{\odot}$, higher than the mass given by Martin & Mignard (1998) (0.705 $M_{\odot}$), but below the mass 0.95 ± 0.1 given by Duquennoy & Mayor (1991) from the spectroscopic orbit. 85 Peg A does not deviate any more from the proper isochrone, once its high [α/Fe] ratio, its true iron abundance corrected for NLTE effects, and sedimentation of heavy elements, are all taken into account. The problem is with 85 Peg B, which is too massive for its absolute magnitude. The colour $(V-K)$ of 85 Peg B can be derived from the V and K magnitudes of (A+B), V=7.75, K=3.94 (Johnson et al. 1968), the magnitudes V_A= 5.81 and V_B= 9.0, and assuming that $(V-K)_A = 1.59 \pm 0.02$ from its effective temperature and Alonso calibration of $(V-K)$ versus (T_{eff}, [Fe/H]). The result is $(V-K)_B$= 3.46 $\pm$0.06, corresponding to about T_{eff} = 3950 K. The associated mass and absolute bolometric magnitude are respectively 0.54 (smaller than the dynamical mass of about 0.7 to 0.8 $M_{\odot}$) and 8.0. With a bolometric correction of -1.1 and the transformation from apparent to absolute magnitudes this gives V_B = 9.57 too faint by 0.6 magnitude. One possibility is that 85 Peg B is a spectroscopic binary itself, but we shall leave this hot subject for another paper, this one having at least clarified the case of 85 Peg A.

7.3. η Cas

Nothing really new, not already in Fernandes et al. (1998), can be said for this star. The fact that it is more evolved introduces one more parameter (age) and prevents to check the unevolved position of the star. The star is nevertheless identified in Fig. 2, and does not raise a particular problem.

8. How does helium content vary with metallicity?

Our isochrones are computed with the assumption that the helium content varies in proportion with metallicity, namely:

$$Y(Z) = Y_{\mathrm{p}} + (Z/Z_{\odot})\,(Y_{\odot} - Y_{\mathrm{p}}) \quad (1)$$

Any unevolved star presenting a significant deviation with respect to the isochrone corresponding to its metallicity may indicate that its helium content deviates from this simple, naive assumption. Actually there is already an indication that the Hyades do not follow this rule (Perryman et al. 1998), Hyades stars being metal-rich by 0.15 dex with respect to the Sun, without being correspondingly helium-rich. On the contrary, the metal-rich stars of the α Cen system were found also helium-rich (Y=0.30) by Fernandes & Neuforge, (1995) in agreement with Eq. (1).

In Fig. 6 we have plotted the most unevolved stars ($M_{\mathrm{bol}} > 5.2$), labeled by their value of [Fe/H], with a solar ZAMS and a grid of isochrones of 8 Gyr, of metallicities -0.3, 0. and $+0.3$. Only stars of metallicity corresponding to this interval are plotted. We admit that the age of these thin disk stars is between 0 and 8 Gyr. So if the error bars intersect either the right metallicity ZAMS or a right metallicity isochrone there is no compelling evidence that the scaled helium value is wrong. Globally all stars within the metallicity range -0.3 < [Fe/H] < 0.3 are within the corresponding isochrones. But inside the lane they define, some stars are not located exactly where one would expect to see them. We note that 5 stars (HD 37394, HD 131977, HD 166620, HD 201091 A, HD 219134) with metallicity very close to zero or even slightly negative, stand on the [Fe/H] = +0.3, 8 Gyr

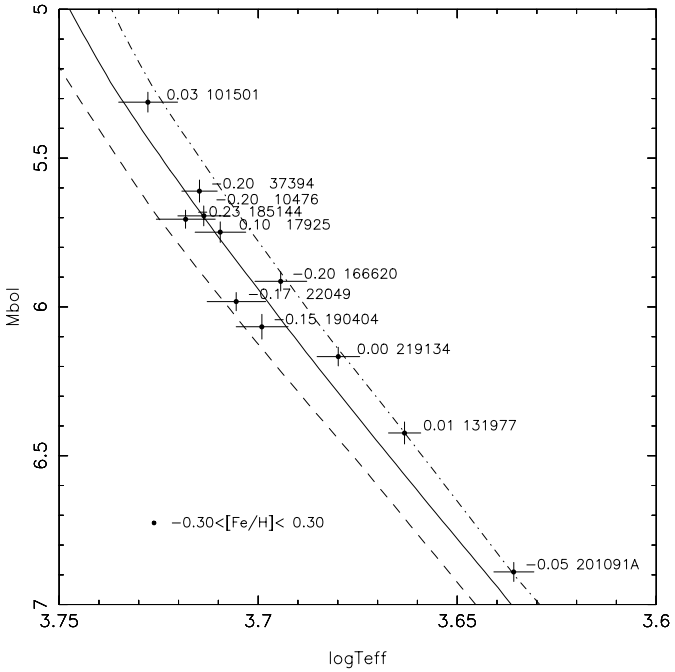

Fig. 6. This figure is a large scale HR diagram for the subsample of unevolved stars in the LTE metallicity range -0.3 < [Fe/H] < 0.3. Each star is labeled by its LTE [Fe/H] value, followed by the HD number of the star. The full line is a standard isochrone for the metallicity [Fe/H] = 0. The dashed line is the standard isochrone corresponding to the LTE metallicity of the sample [Fe/H] = -0.3 The dot-dashed line corresponds to an isochrone of metallicity +0.3. All isochrones are for an age of 8 Gyr, but evolutionary effects are very small, and age is almost irrelevant. If stars stand between the limit isochrones, they do not always closely match the isochrone corresponding to their metallicity, leaving the impression that $\Delta Y/\Delta Z$ is not constant in the sample.

isochrone. The non-LTE correction for their iron abundance is negligible at this metallicity.

As disk stars are younger than halo ones, sedimentation is less important. Its effect has been estimated, using a 5 Gyr, 0.8 $M_{\odot}$ star of solar composition as a template. In this star, the shift in the HR diagram due to microscopic diffusion is of approximately 50 K in effective temperature and 0.02 dex in luminosity. These values are comparable to the observational error bars on these parameters for individual objects. Only for the oldest and more massive stars, the shift can reach more important values, around 120 K. Unfortunately, ages are most of the time unknown for individual *unevolved* stars of the disk.

Though certainly responsible for a scatter in the HR diagram (due to mass and age differences), and for a systematic very small shift towards lower effective temperature, any clear signature of this effect in the data seems impossible to decifer presently. Further work is planned on this point.

Young stars should not show this effect. Indeed, in another paper (Perrymann et al.1998, the content in helium of the Hyades, sufficiently young to forget about diffusion, has been determined, and found to be solar like or slightly below, but certainly not enhanced at the level of the 0.15 dex level of [Fe/H]. Also the very young active stars as ϵ Eridani (HD 22049) or HD 17925 do not significantly deviate from the solar ZAMS.

Another possibility for the 5 stars close to the +0.3 dex isochrone is that these stars have less helium than the scaled value given by Eq. (1). Interpolation of ZAMSs corresponding to various (Y,Z) combinations could provide an estimate of Y, for a star of known Z. However we must remember that the error bar of 0.1 dex on [Fe/H] translates into an error of 0.015 in Y, because of the (Y,Z) degeneracy in the HR diagram. Therefore we have decided to refrain from giving an helium content for individual unevolved stars until the effects of sedimentation are properly quantified at high metallicities.

Summarizing, our data are consistent with the scaled helium content relationship at a coarse level of accuracy, of the order of a factor of two in metallicity, but suggest that a scatter exists at a finer resolution.

9. Conclusions

The location in the ($\log T_{\rm eff}$, $M_{\rm bol}$) plane of a sample of over one hundred nearby stars, covering a metallicity range of $-1.0 < [{\rm Fe/H}] < +0.3$, with Hipparcos parallaxes of relative accuracy better than 5 per cent, has been obtained. Most stars have bolometric magnitudes directly measured, and effective temperatures derived from the Infra-Red Flux Method, by Alonso et al. (1996a). The metallicities (LTE) have been derived from the 1996 edition of the catalogue of $[{\rm Fe/H}]$ determinations by Cayrel de Strobel et al. (1997).

The HR diagram shows an unexpected clumping of stars of low metallicity, only slightly separated from the solar metallicity sequence, as found much earlier, from ground-based parallaxes by Perrin et al. (1977). However the explanation of this fact by a variation of the helium content with metallicity $\Delta Y/\Delta Z = 5.5$ is no more tenable, with the narrow range of variation of Y between $Y_{\rm p} \approx 0.24$ and $Y_{\odot} \approx 0.28$. A comparison of the data with the standard theoretical isochrones, computed with improved opacities, show that unevolved stars with solar metallicities agree more or less with the theoretical expectations, whereas stars with metallicities below -0.5 dex deviate from the isochrones having the same metallicity. The case of μ Cas, a binary of metallicity -0.7, is particularly illustrative.

Two effects, recently studied in the literature have been investigated to explain this observation. The first one concerns only the atmosphere of the star. Until now, non-LTE abundances for iron were not currently available in the literature. Thévenin & Idiart (1999) have studied more than one hundred stars, including μ Cas and many other metal-poor stars, and found a non-LTE correction of +0.15 dex for $[{\rm Fe/H}]$ in μ Cas. Morel & Baglin (1999) have studied the microscopic diffusion of helium and heavier elements in metal-poor stars of various mass. They found that the atmosphere is depleted in iron after 10 Gyr, and that the effective temperature of the star is shifted by about -30 to -200 K for its luminosity. The combination of the two effects brings μ Cas back on its theoretical sequence. The bulk of the combined correction is due to the fact that both the non-LTE correction, and the diffusion of heavy elements, make the at-

mospheric LTE iron abundance not representative of the mean inside abundance of iron.

Among stars with metallicities closer to the solar metallicity there is a global agreement between the observations and the isochrones with a scaled helium abundance, although some scatter may be present. New computations of sedimentation at these metallicities would be necessary to further resolve this issue.

Also an enlarged sample of stars, with distances known with an accuracy of 1 or 2 per cent, appears necessary for a good determination of the helium content of individual stars. The GAIA mission is very promising in this respect (Perryman et al. 1997). With GAIA the mean precision on parallax measurements will be at the 10 micro-arc-second (mas) level up to V=15, to be compared with 1 mas with Hipparcos up to V=9. In parallel, progresses in the analyses of stellar spectra are relevant, as exemplified by the introduction of departures from LTE of the iron atom.

More stellar masses are also deeply needed, not a single mass being known for stars more metal-poor than μ Cas.

Acknowledgements. JF is supported by JNICT (BPD/9919/96). This work was partially supported by the France-Portugal co-operation (project 059-B0). We gratefully thank Pierre Morel for his help with CESAM, and H.-G. Ludwig for having made available results prior to publication. MNP is grateful to R. Canavaggia (†) for her help in the selection of target stars of the Hipparcos proposal 132.

References

Alexander D.R., Ferguson J.W., 1994, ApJ 437, 879
Allen C.W., 1976, Astrophysical Quantities. Athlone Press, London
Alonso A., Arribas S., Martínez-Roger C., 1995, A&A 297, 197
Alonso A., Arribas S., Martínez-Roger C., 1996a, A&AS 117, 227
Alonso A., Arribas S., Martinez-Roger C., 1996b, A&A 313, 873
Axer M., Fuhrmann K., Gehren T., 1994, A&A 291, 895
Balbes M.J., Boyd R.N., Mathews G.J., 1993, ApJ 418, 229
Bikmaev I.F., Bobritskij S.S., El'kin V.G., et al., 1990, In: Michaud G., Tutukov A., Bergevin M. (eds.) Posters presented at the 145th Symposium of the IAU, p. 3
Blackwell D.E., Shallis M.J., 1977, MNRAS 180, 177
Böhm-Vitense E., 1958, Z. Astrophys. 54, 114
Brun A.S., Turk-Chièze S., Morel P., 1998, ApJ 506,913
Carney B.W., Latham D.W., Laird J.B., Aguilar L.A., 1994, AJ 107, 2240
Castellani V., Ciacio F., Degl'Innocenti S., et al., 1997, ApJ 322, 801
Caughlan G.R., Fowler W.A., 1988, Atomic Data Nuc. Data Tables 40, 284
Cayrel R., Lebreton Y., Perrin M.-N., et al., 1997, In: Hipparcos Venice '97, ESA SP-402, 219
Cayrel de Strobel G., Soubiran C., Friel E.D., et al., 1997, A&AS 124, 1
Chaboyer B., Demarque P., Kernan P.J., et al., 1998, ApJ 494, 96
Christensen-Dalsgaard J., 1982, MNRAS 199, 735
Christensen-Dalsgaard J., 1991, In: Gough D.O., Toomre J. (eds.) Challenges to theories of the structure of moderate-mass stars. Springer-Verlag, 11
Cox A.N., Guzik J.A., Kidman R.B., 1989, ApJ 342, 1187
Drummond J.D., Christou J.D., Fugate R.Q., 1995, ApJ 450, 380
Duquennoy A., Mayor M., 1991, A&A 248, 485
Eggleton P.P., Faulkner J., Flannery B.P., 1973, A&A 23, 325
Faulkner J., 1967, ApJ 147, 617
Fernandes J., Lebreton Y., Baglin A., 1996, A&A 311, 127
Fernandes J., Lebreton Y., Baglin A., et al., 1998, A&A 338, 455
Fernandes J., Neuforge C., 1995, A&A 295, 678
Fuhrmann K., Axer M.K., Gehren T., 1995, A&A 301, 492
Fuhrmann K., 1998, A&A 338, 161
Grevesse N., Noels A., 1993, In: Prantzos N., Vangioni-Flam E., Cassé M. (eds.) Origin and Evolution of the Elements. Cambridge University Press
Hogan C.J., Olive K.A., Scully S.T., 1997, ApJ 489, L119
Høg E., Pagel B.E.J, Portinari L., et al., 1997, In: Prantzos N., Tosi M., von Steiger R. (eds.) Primordial Nuclei and their Galactic Evolution. ISSI, Bern, Sp. Sc. Rev., in press
Iglesias C.A., Rogers F.J., 1996, ApJ 464, 943
Izotov Y.I., Thuan T.X., Lipovetsky V.A., 1997, ApJS 108, 1
Johnson H.L., Mitchell R.I., Iriarte B;, Wiśniewski W.Z., 1966, Communication of the Lunar and Planetary Laboratory No. 63, Vol. 4, Part 3, University of Arizona, USA
Johnson H.L., Macarthur J.W., Mitchell R.I., 1968, ApJ 152, 465
Kornneef J., 1983 ApJS 51, 489
Kurucz R.L., 1991, In: Crivarelli L., Hubeny I., Hummer D.G. (eds.) Stellar atmospheres: Beyond Classical Models. NATO ASI Series C, Vol. 341
Lebreton Y., Perrin M.-N., Fernandes J., Cayrel R., Cayrel de Strobel G., Baglin, A., 1997, In: Hipparcos Venice '97, ESA SP-402, 231
Lebreton Y., 1999, In: Livio M. (ed.) May 98 STScI Symposium on Unsolved Problems in Stellar Evolution. CUP, p. 107
Lebreton Y., Däppen W., 1988, In: Proc. Symp. Seismology of the Sun and Sun-like Stars. Tenerife, Spain, ESA SP-286, 661
Lebreton Y., Fernandes J., Cayrel R., 1998, A&A, to be submitted
Lebreton Y., Gómez A.E., Mermilliod J.C., et al., 1997, In: Hipparcos Venice '97, ESA SP-402, 231
Ludwig H.-G., Freytag B., Steffen M., 1999, A&A 346, 111
Maeder A., 1974, A&A 32, 177
Maeder A., 1992, A&A 264, 105
Martin C., Mignard F., 1998, A&A 330, 585
Morel P.J., 1997, A&AS 124, 597
Morel P., Baglin A., 1999, A&A 345, 156
Morel P., van't Veer C., Provost J., et al., A&A 286, 91
Nissen P.E., Høg E., Schuster W.J., 1997, In: Hipparcos Venice '97, ESA SP-402, 225
Noels A., Grevesse N., Magain P., et al., 1991, A&A 247, 91
Pagel B.E.J., Simonson E.A., Terlevich R.J., et al., 1992, MNRAS 255, 325
Pagel B.E.J., Portinari L., 1998, MNRAS 298, 747
Pérez Hernández F., Christensen-Dalsgaard J., 1994, MNRAS 267, 111
Perrin M.N., Hejlesen P.M., Cayrel de Strobel G., et al., 1977, A&A 54, 779
Perryman M., Lindengren L., Turon C., 1997, In: Hipparcos Venice '97, ESA SP-402, 743
Perryman M., Brown A.G.A., Lebreton Y., et al., 1998, A&A 331, 81
Proffitt C.R., Vandenberg D.A., 1991, ApJS 77, 473
Renzini A., 1994, A&A 285, L5
Richard O., Vauclair S., Charbonnel C., Dziembowski W.A., 1996, A&A 312, 1000
Thévenin F., Idiart T., 1999, ApJ 521, 753
Thuan T.X., Izotov Y.I., 1998, In: Prantzos N., Tosi M., von Steiger R. (eds.) Primordial Nuclei and their galactic evolution. Kluwer Academic Publishers, p. 83
Wheeler J.C., Sneden C., Truran J.W., 1989, ARA&A 27, 279
Zahn J.P., 1992, A&A 265, 115